Caccamo P., Naaim-Bouvet F. and Faug T. Influence of upstream catching dam slope on powder avalanche. International Snow Science Workshop (ISSW 2013), Grenoble - Chamonix Mont-Blanc, 7-11 october 2013. pp. 788-793

Influence of upstream catching dam slope on powder avalanche

Caccamo P.*, Naaim-Bouvet F. and Faug T.

ABSTRACT: The influence of an obstacle on the dynamics of a finite-volume density current modelling a powder-snow avalanche was investigated. A constant volume of a dyed salt solution reproduced the small-scale aerosol flowing down an inclined channel immersed in a water tank. Reference tests in the absence of the obstacle characterized the dynamics parameters of the flow and then the influence of two types of obstacles on these parameters was studied. Both of the obstacles represent a catching dam, one with a vertical uphill face (OBS1), and the second one with an inclined uphill face (OBS2). A high resolution acoustic velocimeter allows measurements on the 3D flow velocity. For the reference avalanche, it was shown that the maximum velocity norm can be up to 18% greater than the maximum horizontal contribution (parallel to the slope). In terms of protection effectiveness, laboratory tests showed that a catching dam with the upstream face vertical to the slope is more efficient than a dam with an inclined upstream face. In presence of OBS2 the flow does not hit the obstacle but it rather passes smoothly over it, without any visible detachment from the surface. The ramp effect is remarkable and the avalanche reaches in a shorter time a given point downstream from the obstacle. On the contrary, in the OBS1 configuration, the incoming flow hits the vertical wall and bursts. The flow is subjected to a strong deflection with the formation of a vertical jet.

KEYWORDS: powder snow avalanche, density current, water tank, catching dam, 3D acoustic velocimeter.

1 INTRODUCTION

An aerosol avalanche is a turbulent flow resulting from the suspension of snow particles in the air. It appears to be a big snow cloud travelling at a very high velocity (Beghin and Olagne, 1991; Nishimura et al., 1995). This type of flow usually originates from a dense avalanche. For powder snow, the majority of researchers suggest that, in the presence of cold dry snow with a low cohesion rate, the avalanche must reach a velocity of 10 m s^{-1} before the air forms a snow cloud (Beghin and Olagne, 1991; Hopfinger, 1983). More cohesive types of snow can also generate an aerosol, but the velocity necessary for forming the cloud would be higher.

An aerosol avalanche is composed of a turbulent-eddy structure moving rapidly and increasing its volume until it exceeds a height of several dozen metres. The snow density greatly varies. Table 1 summarizes the typical values for the aerosol layer of an avalanche.

Table 1: Typical values for the characteristic parameters of a powder snow avalanche (Issler, 2010).

Density (kg m^{-3})	$1 - 10$
Particle density (kg m^{-3})	900
Volume fraction ()	< 0.01
Particle diameter (mm)	< 1
Velocity (m s^{-1})	$20 - 100$
Height (m)	$10 - 100$
Pressure (kPa)	$1 - 20$

In the domain of avalanche protection design, defence structures are built mainly to stop the dense part of an avalanche. The aerosol part does not follow the terrain morphology and generally overtakes the obstacle. The aim is to quantify the residual risk that this phenomenon still represents downstream from the protection structure. The present paper is devoted to an experimental laboratory study of this question in snow avalanche engineering.

Small-scale tests date back to the 1970s and have developed over three main axes using different principles: *(i)* a heavy fluid flowing in a lighter fluid (Beghin, 1979; Beghin and Olagne,

* *Corresponding author address:* Caccamo P., Irstea, UR ETGR, 2 rue de la Papeterie - BP 76, F-38402 Saint-Martin-d'Hères, France,
Email: paolo-caccamo@libero.it

Caccamo P., Naaim-Bouvet F. and Faug T. Influence of upstream catching dam slope on powder avalanche. International Snow Science Workshop (ISSW 2013), Grenoble - Chamonix Mont-Blanc, 7-11 october 2013. pp. 788-793

1991; Hopfinger and Tochon-Danguy, 1977), *(ii)* bi-phase simulations with water (Hermann and Hutter, 1991; Rastello, 2002) and *(iii)* bi-phase simulations with air (Bozhinskiy and Sukhanov, 1998; Nishimura et al., 1998; Turnbull and McElwaine, 2008, 2010).

Aerosol avalanche field experiments are very complex and, at the moment, not widely developed and potentially dangerous. However, even if new technologies and measurement techniques have been developed, there remains very limited understanding of the interaction between a powder-snow avalanche and an obstacle. Little research has investigated this interaction on small-scale laboratory models. The pioneering studies belong to Hopfinger and Tochon-Danguy (Hopfinger and Tochon-Danguy, 1977). For slopes equal to or greater than 10°, first Beghin and Closet (Beghin and Closet, 1990) and then Augé (Auge et al., 1995) performed experimental tests with unsteady flows striking deviation and catching dams in 2D and 3D configurations. Keller and Issler (Keller, 1996) also investigated the influence of obstacles on the dynamics of an aerosol avalanche, and they evaluated the effectiveness of retarding and deviating dams. These research works (except for Keller and Issler) mainly concerned measurements of the front velocity of the avalanche cloud. Innovative studies were done by Naaim-Bouvet et al. (2002) who used ultrasonic Doppler velocimetry to measure the avalanche velocity in the cloud.

Small-scale laboratory tests greatly enhance the general understanding of powder avalanches. In the present paper this approach was adopted.

Section 2 details the experimental procedure and the measurement techniques. The data from experiments are discussed in section 3 with a focus on the qualitative results and, lastly, section 4 concludes this paper and proposes some insight into future works.

2 EXPERIMENTAL APPROACH

In this work, small-scale experiments were conducted using a heavy fluid flowing in a lighter fluid. Powder-snow avalanches were modelled as density clouds obtained through a finite-size volume of dyed salt solution flowing into water. Tests were performed in different set-up configurations and aimed to investigate the dynamics of a buoyant cloud and its behaviour upon interaction with an obstacle. Attention was focused on the influence of two catching dams on the dynamics of a quasi-2D aerosol flow, and, in particular, on the influence of the uphill slope of the dam on the protection effectiveness. This topic is relevant because it is directly related to engineering and costs issues. An inclined uphill face of $\alpha_{dam} = 32^{\circ}$ corresponds to the natural angle of repose for an earth-filled dam and thus, from an engineering point of view, it represents a much simpler and low-cost solution for the construction of a dam.

Table 2: Dimensionless numbers

	Reality	Small-scale model
Re	10^8	10^4
Fr_d	0.5	0.5
$\frac{\Delta\rho}{\rho_{ref}}$	$4-10$	0.2

2.1 Froude scale modelling

Small-scale modelling must meet similitude requirements to provide results that can be used for the study of the real-scale phenomenon. The Froude-scale modelling is based on a similitude approach in which the current is fully characterised by a series of dimensionless variables (Kneller and Buckee, 2000). The dimensional analysis identifies the number of dimensionless parameters representing all of the variables controlling the system. In small-scale powder avalanche modelled by a density current, these parameters are:

1. The Reynolds number, $Re = \frac{\rho u L}{\eta_d}$, which represents the contribution of inertial on viscous forces, where ρ is the flow density, u is its mean velocity, L is a characteristic dimension and η_d is the fluid dynamic viscosity;
2. The densimetric Froude number, $Fr_d = \frac{u}{\sqrt{\frac{\Delta\rho}{\rho_{ref}} g h}}$, which reflects the ratio of inertial to gravitational forces acting on the flow (h is the flow height);
3. The density ratio, $\frac{\Delta\rho}{\rho} = \frac{\rho - \rho_{ref}}{\rho_{ref}}$, representing the density difference between the two fluids adopted (ρ is the aerosol density and ρ_{ref} the ambient fluid density)

Table 2 gives the typical values of these three dimensionless parameters for real powder-snow avalanches and small-scale tests presented in this paper. The Reynolds number is very high for both cases, which means fully turbulent flows and thus the similitude requirement regarding Re

Caccamo P., Naaim-Bouvet F. and Faug T. Influence of upstream catching dam slope on powder avalanche. International Snow Science Workshop (ISSW 2013), Grenoble - Chamonix Mont-Blanc, 7-11 october 2013. pp. 788-793

is relaxed. The densimetric Froude number is respected but the density ratio is not conserved. A very high velocity is necessary in order to achieve both requirements in laboratory tests, which means that an experimental device of huge dimensions is required. In the 1980s, at the beginning of physical modelling, this was not considered as a serious deficiency (Beghin and Closet, 1990; Beghin and Olagne, 1991; Scheiwiller et al., 1987). However, the relative difference in density might have a reducing effect on the entrainment rate of the ambient fluid (Hopfinger and Tochon-Danguy, 1977). In the 2000s, due to the improvement of technical instrumentation, the numerical modelling of physical simulations was carried out, allowing the numerical simulation of the flow behaviour for higher density ratios (2, 5 and 10). Moreover, recent experimental devices (Turnbull and McElwaine, 2008) allowed the density ratio requirement to be respected.

2.2 The device

The experiments were carried out in a 4 m $\times$ 2.5 m $\times$ 2 m water tank with glass walls. An inclined channel of 2.6 m long and 0.3 m wide has been installed inside of the water tank. The channel slope has a constant incline of 13°, representing the average slope of the study area. By opening the reservoir gate, 4 litres of fluid are released and start flowing along the channel. A reference system is set here and is used in the following. As shown in Figure 1.*a*, the x-axis corresponds to the channel axis, and $x = 0$ is set at the release gate. The z-axis is normal to the channel bottom and to the flow direction, and $z = 0$ corresponds to the channel bottom. The y-axis, consequently, is defined normal to the x and $z-$axis.

Powder-snow avalanches are simulated by a heavy fluid dispersing in a lighter fluid. The heavy fluid consists of dyed salt water. Salt water in saturated conditions has a density of 1185 kg m^{-3}, which rises a value of $\rho = 1200$ kg m^{-3} when the kaolin is added. A finite volume of fluid is released quasi-instantaneously from the immersed reservoir generating an unsteady density cloud. A catching-dam-like obstacle was installed at a distance of 1 m from the releasing gate. Two obstacles were tested, placed perpendicular to the channel axis and to the flow main direction in order to span the entire width of the channel. The first dam ($OBS1$) has a triangular cross-section representing the shape and the dimension ratios of a classic earth-filled protection

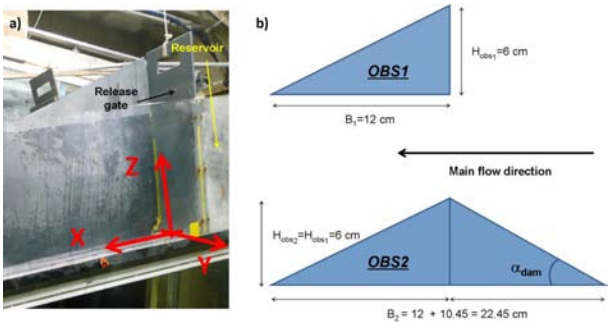

Figure 1: *(a)* Part of the immersed inclined channel and the reference system that is used throughout this paper. The x-axis corresponds to the channel axis, and $x = 0$ is set at the release gate. The z-axis is normal to the channel bottom and to the flow direction, $z = 0$ corresponds to the channel bottom. The y-axis, consequently, is defined normal to the x and $z-$axis. *(b)* Dams' cross-sections.

structure. The second structure ($OBS2$) aims to reproduce a dam where the uphill wall is not vertical but inclined at an angle $\alpha_{dam} = 32^{\circ}$ with respect to the ground. Figure 1.*b* shows the two structure's cross-sections.

Two Canon $XL1$ video cameras with a recording frequency of 25 fps were placed on the channel side with their longitudinal axis perpendicular to the channel and the transversal axis parallel to the flow direction in order see the avalanche flowing horizontally. The two video cameras were placed with their fields of view overlapping in order to ensure continuity between measurements obtained from the uphill and downhill cameras. An acoustic velocimeter measuring the $3D$ velocity field of the density cloud completes the experimental device.

2.3 Measurements techniques

2.3.1 Maximum flow height and front velocity

The maximum flow height (h_{max}) and the front velocity (u_{fr}) were measured by recording t he flow and processing the image sequences (Figure 2.*a*). The image treatment required an accurate calibration (Figure 2.*b*) because images are affected by a potentially significant deformation of the lens of the video camera (Caccamo, 2008).

2.3.2 Core velocity

Core velocity was found to be higher than the front velocity (Hopfinger and Tochon-Danguy,

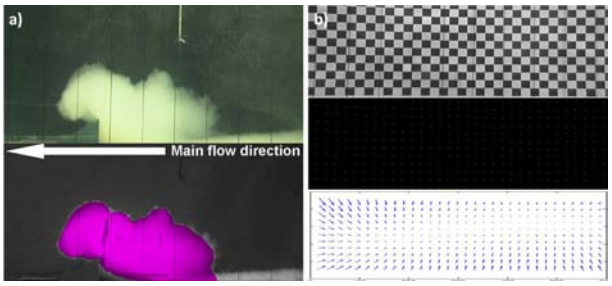

Figure 2: *(a)* Visual restitution of the image processing (the Vectrino beam is visible in the upper image). *(b)* Calibration steps: the checker-pattern is recorded, intersection points are detected and the deformation rate is calculated and associated to all the intersection points.

1977; Keller and Issler, 1996; Naaim-Bouvet et al., 2002) and, due to turbulence eddies, the maximum velocity values were found inside of the cloud. To measure the core velocity, the Vectrino Doppler velocimeter was used. It is a high resolution acoustic velocimeter used to measure turbulence and $3D$ water velocity on a wide variety of applications from the laboratory to ocean. This uses the Doppler effect to measure currents velocity by transmitting a short pulse of sound, listening to its echo and measuring the change in pitch or frequency of the echo. Measurements were taken at different positions along the x-axis ($y = 0$). Positions were calculated with respect to the releasing gate (x_0) and ranged between $x = 0.5$ m and $x = 1.9$ m. The obstacle was placed at $x = 1$ m. At a fixed x-position, vertical profiles of velocities ($u(z)$) were achieved by positioning the sensor at different heights with respect to the bottom of the channel. Typically, a height ranging from 0 to 20 cm (30 cm around the obstacle) was investigated through 9 to 13 distinct z-values. For a fixed position (x;$y = 0$;z), three to five tests were repeated and their results were averaged.

A typical output obtained from Vectrino measurements is shown in Figure 3.

3 EXPERIMENTAL RESULTS

Three measurement campaigns were carried out for the three different configurations. The reference conditions (REF) were tested the first, in order to characterize the flow dynamics in the absence of the obstacle. Then $OBS1$ was mounted, and finally $OBS2$ replaced it. The flow maximum height and its front velocity were measured by image processing and the Vectrino provided the data

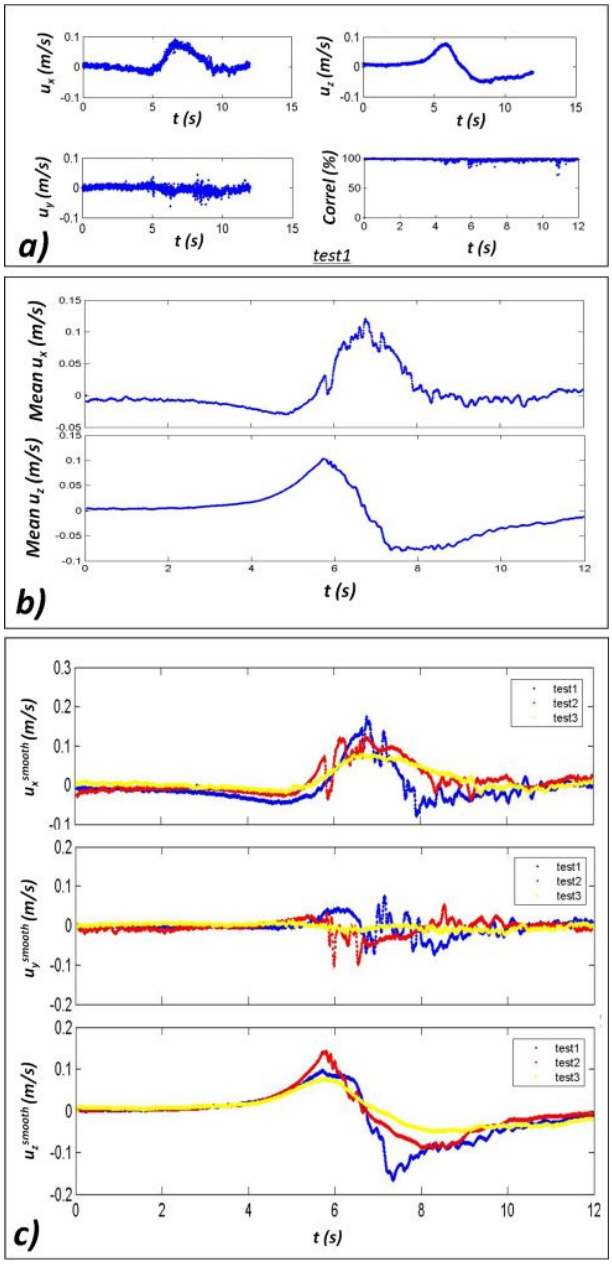

Figure 3: Typical output from Vectrino measurements. The example was taken at $x = 1.30$ m and $z = 19$ cm in the OBS2 configuration. *(a)* Typical profiles obtained from a test (test1). Low-correlation and aberrant data were removed. *(b)* Final mean profiles for u_x and u_z. *(c)* Comparison of smoothed profiles.

Caccamo P., Naaim-Bouvet F. and Faug T. Influence of upstream catching dam slope on powder avalanche. International Snow Science Workshop (ISSW 2013), Grenoble - Chamonix Mont-Blanc, 7-11 october 2013. pp. 788-793

concerning the $3D$ velocity field of the flow. Thanks to these values, the maximum core velocity norm U_{xz}^{max} could be derived as well as the associated angle α_{xz}^{max} which defines the norm direction. The presence of an obstacle systematically influences the flow dynamical parameters. At the impact with the dam:

- the maximum height h_{max} increases,
- the front velocity u_{fr} decreases (then it starts increasing again but without attaining the reference values),
- the maximum horizontal core velocity U_x^{max} decreases,
- the maximum velocity norm U_{xz}^{max} decreases (except for the $OBS2$ configuration).

When dealing with the flow dynamic characteristics, the maximum core velocity norm U_{xz}^{max} is a more precise parameter to take into account, rather than U_x^{max}. Results showed that, in reference conditions, the maximum norm can be up to 18% greater than the maximum horizontal contribution. This is remarkable when considering that the impact pressure is proportional to the velocity square.

However, when comparing the effectiveness of the two different catching dam solutions ($\alpha_{dam} = 90^{\circ}$ and $\alpha_{dam} = 32^{\circ}$, results showed that the $OBS2$ (inclined upstream face solution) has a lower influence on the flow dynamical behaviour with respect to a catching dam with a vertical uphill face ($OBS1$). Figure 4 gives a visual overview of the flow behaviour for the three configurations at three different front positions, uphill from the obstacle ($x_{fr} \simeq 0.85$ m), around the obstacle ($x_{fr} \simeq 1.2$ m) and downhill from the obstacle ($x_{fr} \simeq 1.8$ m).

Reference flows flow down the channel with a velocity that appears to be rather constant. Their turbulent structure develops into a series of eddies rotating clockwise of different dimensions. In the $OBS1$ configuration, the incoming flow hits the vertical wall of the dam and bursts. The cloud height rapidly increases, the front of the flow separates into two main parts, an upper part rotating clockwise expanding upward and a second part generating new eddies turning counter-clockwise. The impact with the obstacle makes the cloud incorporate the ambient fluid, its surface increases and thus its density, theoretically, decreases. The flow is subjected to a strong deflection with the formation of a vertical jet. In the presence of the second dam configuration ($OBS2$), a different behaviour was observed. The flow does not hit the obstacle, but rather it passes smoothly over it, without any visible detachment from the surface. The obstacle seems to not be very efficient in terms of flow energy reduction.

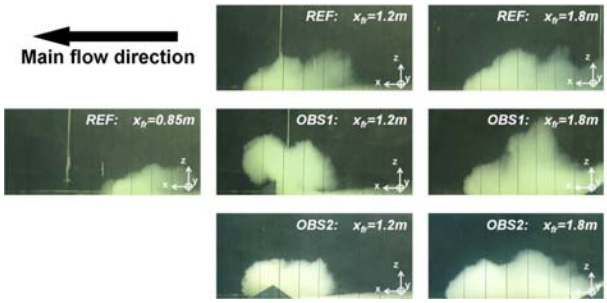

Figure 4: Visual overview of the flow behaviour at three different channel sections and for the three investigated configurations. The flow behaviour is supposed to be similar for all the configurations far uphill from the obstacle (section at $x_{fr} = 0.85$ m).

These observations qualitatively resume the results obtained from small-scale laboratory tests.

4 CONCLUSION AND OUTLOOK

This work investigated the influence of an obstacle on the dynamics of a finite-volume density current likely to mimic a powder-snow avalanche. A constant volume of a dyed salt solution reproduced the small-scale aerosol flowing down an inclined channel ($\theta = 13^{\circ}$) immersed in a water tank. Reference tests, in the absence of the obstacle, characterised the dynamics of the flow and then the influence of two different types of obstacles on these parameters was investigated. Both of the obstacles represent a catching dam. $OBS1$ has a vertical uphill face ($\alpha_{dam} = 90^{\circ}$) while $OBS2$ has an inclined uphill face ($\alpha_{dam} = 32^{\circ}$). Measurements were taken for the maximum flow height and on the front and core velocity by using image processing and the ultrasound Doppler velocimetry.

Small-scale modelling of powder snow avalanches showed that a catching dam with an uphill face inclined at an angle $\alpha_{dam} = 32^{\circ}$ is much less efficient to reduce the energy of an aerosol flow than a dam with an uphill face normal to the terrain slope. This experimental configuration can easily occur in reality. As previously mentioned, this angle corresponds to the natural angle of repose for an earth-filled dam and thus represents an easier and less expensive design solution. Moreover, the deposit from a previous avalanche, stored uphill from the vertical wall, can

Caccamo P., Naaim-Bouvet F. and Faug T. Influence of upstream catching dam slope on powder avalanche. International Snow Science Workshop (ISSW 2013), Grenoble - Chamonix Mont-Blanc, 7-11 october 2013. pp. 788-793

form a ramp for a second incoming event.

From an engineering point of view, it would be interesting to calculate the equivalent height of a dam with an inclined uphill face necessary for reaching the same effectiveness of a dam with a vertical uphill face. Lastly, in order to apply the experimental results obtained in the small-scale water tank to real case studies, numerical simulations should be conducted to correct the density distortion affecting laboratory data. However, these data already provided a good benchmarking database for future numerical simulations.

Acknowledgements: this study received financial support mainly from the European project Dynaval (INTERREG-ALCOTRA). The authors would like to thank Hervé Bellot and Frederic Ousset for their crucial contribution to the experimental set-up and the data acquisition.

5 REFERENCES

Auge, A., Ousset, F., Marco, O., 1995. Effet d'une digue sur l'écoulement d'un aerosol. The contribution of scientific research to safety with snow, ice and avalanche , 235–240.

Beghin, P., 1979. Etude des bouffées bidimensionelles de densité en écoulement sur pente avec application aux avalanches de neige poudreuse. Ph.D. thesis. Institut National Polytechnique de Grenoble.

Beghin, P., Closet, J.F., 1990. Effet d'une digue sur l'écoulement d'une avalanche poudreuse. Notes Techniques du Cemagref 77.

Beghin, P., Olagne, X., 1991. Experimental and theoretical study of the dynamic of powder snow avalanches. Cold Regions Science and Technology 19, 317–326.

Bozhinskiy, A.N., Sukhanov, L.A., 1998. Physical modeling of avalanches using an aerosol cloud of powder materials. Annals of Glaciology 26, 242–246.

Caccamo, P., 2008. Experimental assessment of the influence of a dam on powder snow avalanche inpact: the case study of Taconnaz. Master's thesis. Politecnico of Milano.

Hermann, F., Hutter, K., 1991. Laboratory experiments on the dynamics of powder-snow avalanches in the run-out zone. Journal of Glaciology 37, 281–295.

Hopfinger, E.J., 1983. Snow avalanche motion and related phenomena. Annual Review of Fluid Mechanics 15, 47–76.

Hopfinger, E.J., Tochon-Danguy, J.C., 1977. A model study of powder-snow avalanches. Journal of Glaciology 19, 343–356.

Issler, D., 2010. Dynamique et modélisation des avalanches, in: Université Européenne d'Eté.

Keller, S., 1996. Physikalische simulation von staublawinen - experimente zur dynamik im dreidimensionalem auslauf. VAW, ETH Zürich 141.

Keller, S., Issler, D., 1996. Staublawinen über Dämme und Mauern im Labor; Zusammenstellung aller Resultate und Auswertung. Technical Report. Swiss Federal Institute for Snow and Avalanches.

Kneller, B., Buckee, C., 2000. The structure and fluid mechanics of turbidity currents: a review of some recent studies and their geological implications. Sedimentology 47, 62–94.

Naaim-Bouvet, F., Naaim, M., Bacher, M., Heiligenstein, L., 2002. Physical modelling of the interaction between powder avalanches and defence structures. Natural Hazards and Earth System Sciences 2, 193–202.

Nishimura, K., Keller, S., McElwaine, J., Nohguchi, Y., 1998. Ping-pong ball avalanche at a ski jump. Granular Matter 1, 51–56.

Nishimura, K., Sandersen, F., Kristensen, K., Lied, E., 1995. Measurements of powder-snow avalanche nature. Surveys in Geophysics 16, 649–660.

Rastello, M.C., 2002. Etude de la dynamique des avalanches de neige en aérosol. Ph.D. thesis. Université Joseph Fourier, Grenoble.

Scheiwiller, T., Hutter, K., Hermann, F., 1987. Dynamic of powder snow avalanches. Annales Geophysicae. Series B 5, 569–587.

Turnbull, B., McElwaine, J.N., 2008. Experiments on the non-bousinnesq flow of self-igniting suspension currents on a steep open slope. Journal of Geophysical Research 113, 1–12.

Turnbull, B., McElwaine, J.N., 2010. Potential flow models of suspension current air pressure. Annals of Glaciology 51, 113–122.